

The role of pennation angle and architectural gearing to rate of force development in dynamic and isometric muscle contractions

Bas Van Hooren¹  | Per Aagaard²  | Andrea Monte³  | Anthony J. Blazevich⁴ 

¹Department of Nutrition and Movement Sciences, NUTRIM School of Nutrition and Translational Research in Metabolism, Maastricht University Medical Centre+, Maastricht, The Netherlands

²Department of Sports Science and Clinical Biomechanics, University of Southern Denmark, Odense, Denmark

³Department of Neurosciences, Biomedicine and Movement Sciences, University of Verona, Verona, Italy

⁴Centre for Human Performance, School of Medical and Health Sciences, Edith Cowan University, Joondalup, Western Australia, Australia

Correspondence

Bas Van Hooren, Department of Nutrition and Movement Sciences, NUTRIM School of Nutrition and Translational Research in Metabolism, Maastricht University Medical Centre+, Universiteitssingel 50, Maastricht 6229 ER, The Netherlands.
Email: b.vanhooren@maastrichtuniversity.nl

Abstract

Background: Associations between muscle architecture and rate of force development (RFD) have been largely studied during fixed-end (isometric) contractions. Fixed-end contractions may, however, limit muscle shape changes and thus alter the relationship between muscle architecture and RFD.

Aim: We compared the correlation between muscle architecture and architectural gearing and knee extensor RFD when assessed during dynamic versus fixed-end contractions.

Methods: Twenty-two recreationally active male runners performed dynamic knee extensions at constant acceleration ($2000^{\circ}\text{s}^{-2}$) and isometric contractions at a fixed knee joint angle (fixed-end contractions). Torque, RFD, vastus lateralis muscle thickness, and fascicle dynamics were compared during 0–75 and 75–150 ms after contraction onset.

Results: Resting fascicle angle was moderately and positively correlated with RFD during fixed-end contractions ($r=0.42$ and 0.46 from 0–75 and 75–150 ms, respectively; $p<0.05$), while more strongly ($p<0.05$) correlated with RFD during dynamic contractions ($r=0.69$ and 0.73 at 0–75 and 75–150 ms, respectively; $p<0.05$). Resting fascicle angle was (very) strongly correlated with architectural gearing ($r=0.51$ and 0.73 at 0–75 ms and 0.50 and 0.70 at 75–150 ms; $p<0.05$), with gearing in turn also being moderately to strongly correlated with RFD in both contraction conditions ($r=0.38$ – 0.68).

Conclusion: Resting fascicle angle was positively correlated with RFD, with a stronger relationship observed in dynamic than isometric contraction conditions. The stronger relationships observed during dynamic muscle actions likely result from different restrictions on the acute changes in muscle shape and architectural gearing imposed by isometric versus dynamic muscle contractions.

KEYWORDS

belly gearing, biomechanics, gear ratio, muscle architecture, muscle mechanics, performance

Bas Van Hooren, Per Aagaard, Andrea Monte and Anthony J. Blazevich equally contributed to the study.

This is an open access article under the terms of the [Creative Commons Attribution](https://creativecommons.org/licenses/by/4.0/) License, which permits use, distribution and reproduction in any medium, provided the original work is properly cited.

© 2024 The Authors. *Scandinavian Journal of Medicine & Science In Sports* published by John Wiley & Sons Ltd.

1 | INTRODUCTION

The capacity to rapidly develop force (i.e., exerting a high rate of force development (RFD)) during tasks requiring high muscle shortening velocities is important for success in many sports, and for competent performance in various activities of daily living.^{1,2} While the contribution of neural factors to rapid force production under various conditions is well described,^{2,3} less is known about the possible role of muscle architecture (e.g., pennation angle or fascicle length) and tissue-mechanical properties (e.g., tendon stiffness,^{2,4} contractile and elastic component lengths⁵). Indeed, only a small number of studies have investigated associations between muscle architecture and RFD, and these studies have reported conflicting findings.^{6–11} Consequently, a recent review has concluded that muscle architecture may have a minimal effect on RFD in humans.² However, the relationship between muscle architecture and RFD has typically been investigated during fixed-end contractions (i.e., isometric at the muscle–tendon unit level),^{6–9,11} whereas human movements often involve anisometric contractions linked to dynamic joint rotations. While both isometric and anisometric muscle contraction can induce transverse forces between muscles¹² that in turn restrict shape changes, muscles may more readily change in shape during anisometric contractions than during fixed-end contractions due to the static joint configuration in the latter condition.

Acute changes in muscle shape (including modulations in pennation angle and fascicle length) strongly influence mechanical (i.e., contractile) function and thereby may affect both the force and speed of contraction.^{13–16} Specifically, if muscle fascicles shorten and bulge in the thickness direction, a lateral force will be exerted onto neighboring fascicles, forcing the whole muscle to also expand in the thickness direction. As a result, fascicles rotate about their insertion point at the aponeurosis/tendon, in turn increasing their angle relative to the aponeurosis and increasing whole-muscle thickness while inducing longitudinal muscle shortening (Figure 1). Fascicle rotation (i.e., the change in pennation angle) that occurs during anisometric muscle contractions thereby contributes directly to the overall muscle length change (and hence contraction velocity) in addition to that caused by changes in length of the fascicles themselves.

The contribution of changes in pennation angle to changes in muscle length can be calculated as where Δm is the change in muscle belly length, f is fascicle

$$\Delta m = f_2 \cdot (\cos\alpha_2 - \cos\alpha_1) \quad (1)$$

length, α is the pennation angle, and subscripts 1 and 2 refer to the initial and final positions, respectively.¹⁷ As described

by this relationship (Equation 1), overall muscle origin–insertion shortening distance, and thus speed, may substantially exceed fascicle (or fiber) shortening distance, and speed.^{18–21} This functionally important feature of pennate skeletal muscle has been termed “architectural gearing,” defined as the ratio (architectural gear ratio) between overall muscle shortening velocity and fascicle shortening velocity.^{13,22} The architectural gear ratio has been shown to be >1.0 under various contraction conditions in both animal^{20,23,24} and human experiments,^{10,25,26} although the magnitude of effect depends on the requirements of the task such as the force produced^{20,26,27} (Figure 1) and the rate at which force is produced.²⁸ Furthermore, the gear ratio also depends on the spacing between fascicles²⁷ and material characteristics of the muscle–tendon unit such as the stiffness of connective tissues (i.e., extracellular matrix and aponeurosis^{23,28,29}), where higher connective tissue stiffness may restrict the muscle’s capability to change in shape. Similarly, because longer tendons are more compliant than shorter tendons if cross-sectional area and material properties are similar (e.g., ref. [5]), tendon length per se can also influence gearing. Finally, gearing may also depend on the restrictions in muscle shape change imposed by the specific motor task.³⁰ For example, the continuous change in joint angle during a dynamic concentric contraction may allow for greater muscle shortening and thus greater shape change as opposed to an isometric (fixed-end) contraction. If more restricted shape changes are imposed during fixed-end than dynamic contractions (or vice versa), this is likely to alter the relationship(s) between muscle–tendon architectural and mechanical properties and RFD. This in turn may thus partially explain the conflicting associations between muscle architecture and RFD reported previously.^{4–8}

The primary aim of this study, therefore, was to investigate the relationship between resting muscle architecture and RFD in dynamic and fixed-end contraction conditions, and to compare the strength of this relationship across different contraction conditions. As resting pennation angle has been shown to influence architectural gearing in a segmented muscle model,¹³ we hypothesized that larger resting muscle pennation angles would be associated with higher gear ratios, thereby enabling faster RFD during both isometric and dynamic contractions. The reason for this is that for a given muscle contraction velocity, higher gear ratios were expected to reduce fascicle shortening velocity thereby allowing for greater (rate of) force production according to the force–velocity relationship. Additionally, it was hypothesized that the correlation between resting muscle pennation angle and both gear and RFD would be weaker during isometric than dynamic contractions due to contraction-specific restrictions imposed on muscle shape changes, which in some conditions may limit fascicle rotation and hence reduce

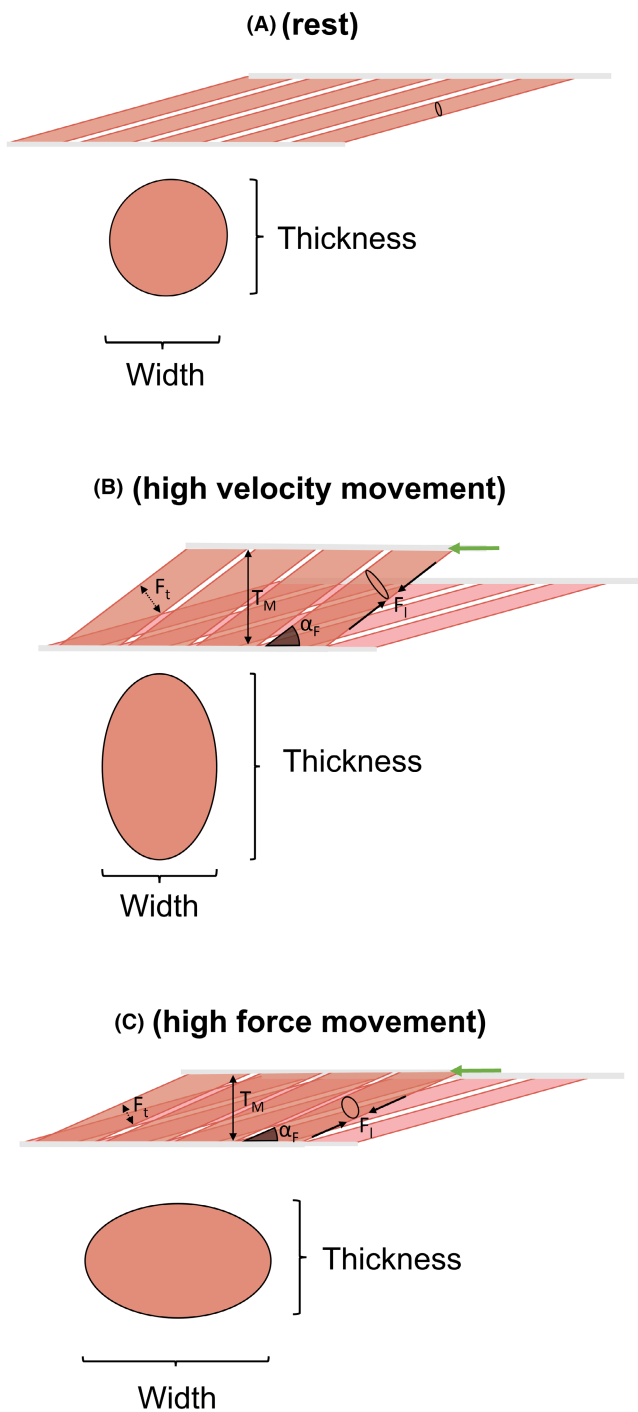


FIGURE 1 (A) Schematic illustration of muscle fascicles in a resting muscle before contraction. (B, C) Concentric muscle contraction causing whole-muscle bulging in the thickness and width directions, respectively. Due to the close packing of fascicles and the shallow fascicle angle at rest (A), there is insufficient space for fascicle bulging. In an idealized deformation scheme whereby the aponeurosis length remains constant, any fascicle bulging in the thickness direction will therefore force the fascicles to rotate to greater angles ($\uparrow\alpha_F$), thereby increasing whole-muscle thickness ($\uparrow T_M$). (C) In contrast, during high-force contractions (i.e., when external loads are high), the longitudinal force exerted by the fascicles (F_L) acts against whole-muscle bulging in the thickness direction, so fascicle and whole-muscle bulging must predominately occur in the width direction (see cross-sections in C). The reduced muscle thickening therefore limits fascicle rotation and contributes to slower whole-muscle shortening (muscle shortening speed is similar to fascicle shortening speeds) (green arrow). Nonetheless, as the fascicles remain more closely aligned with the direction of whole-muscle shortening, a greater proportion of the fascicle force is directed along the tendon, so whole-muscle maximum force is greatest (contractile efficiency is enhanced). This variable gearing capacity, based on muscle forces, allows for increased muscle shortening speeds under low-force contractions (when fascicle rotation is great) yet increases effective (projected) muscle force generation during high load contractions (when fascicle rotation is reduced). Thus, pennate muscles can intrinsically change gears to optimize contractile capacity as the force requirements of a task are changed.

2 | MATERIALS AND METHODS

2.1 | General study design

To test the hypotheses, we used data obtained as part of a larger project investigating the contribution of muscle architectural gearing to mechanical output during rapid dynamic contractions.²⁵ In this project, participants performed a series of maximal, explosive fixed-end (isometric) and dynamic (concentric), knee extensor contractions. During each contraction, vastus lateralis (VL) architectural changes and the knee extensor moment were recorded simultaneously. All experiments were approved by the local ethics committee (protocol number: 2019-UNVRCL-0193291) and conducted in agreement with the declaration of Helsinki.

2.2 | Participants

Twenty-two recreationally active male runners (mean \pm SD age 25 ± 3 years, mass 76 ± 3.5 kg, and height 1.76 ± 0.03 m) volunteered for the study and signed an informed consent form prior to participation. The participants did not report any type of neuromuscular injury during the 6 months preceding the experiments. Pilot experiments showed a

gear (Figure 1). Further, several lines of evidence suggest that fascicle/fiber forces drive the changes in gear,^{20,26,27} with higher gear observed during low-force contractions and lower gear during high-force contractions (Figure 1). Because force production can differ between isometric and dynamic contractions, we compared the relationships between muscle architecture and RFD in the two contractions at a common torque level during early phase (0–75 ms) RFD, and also during a later time window (75–150 ms) where muscle force (torque) differed between conditions.

larger variability in dynamic muscle shape change in females, and therefore, only males were included in this initial experiment.

2.3 | Experimental set-up

The contribution of neural and architectural factors to RFD has typically been investigated during the first 200 ms after contraction onset, due to the importance of RFD within this time window for athletic events and daily life activities.² In this study, we therefore investigated VL behavior in isometric and dynamic contraction conditions during this time window and how differences in this behavior could affect the mechanical output. The knee extensors contractile capability should be similar to ensure a proper comparison between the conditions. To achieve this, each participant was positioned in an isokinetic/isoinertial dynamometer (Biodex, model 3) such that they exhibited comparable knee extensor force capacity during each contraction.

To ensure a similar knee extensor force capacity, we first determined the knee joint angle at which the maximum knee extensor torque could be generated. To this purpose, each participant performed eight maximum voluntary contractions (MVCs) at different fixed knee joint angles (from 90° to 20° where 0° = knee fully extended) with 10° intervals. During each MVC, the participant was asked to push “as hard as possible” for 4 s. Two maximal contractions were performed at each joint angle, with 2 min of recovery in between.

The mean joint angle at which peak torque was produced was estimated to be 65° (see Section 2.5 for more details), and this angle was used for the explosive fixed-end contraction in all participants (see ref. [25]). The explosive dynamic contractions were configured so that the knee angle associated with peak knee extensor torque production was reached half-way within the 150 ms time window for each participant. Since the acceleration profile and angular velocity of the dynamometer and target knee angle all were controlled, the starting knee joint angle was selected so that 75 ms of contraction occurred before and after reaching the target knee angle (Figure S1). To achieve this, the dynamometer lever arm moved slowly (10°s^{-1}) from the maximum knee joint flexion angle to the starting position where the acceleration phase was initiated, in line with previous reports.³¹ At the starting angle, the dynamometer accelerated at a constant acceleration of 2000°s^{-2} and stopped when the knee was fully extended. At the end of these procedures, the VL operated at a comparable F-L potential (i.e., fraction of the maximum force that a muscle could exhibit during a specific contraction) during each contraction type (0.79 and 0.81

for the fixed-end and explosive dynamic contraction, respectively). Further details are reported in Monte et al.²⁵

2.4 | Data collection

Participants performed 15 trials of each contraction condition. In both conditions, the participants were instructed to extend their knee “as fast and as hard as possible” with an emphasis on a “fast”³² contraction effort. During the explosive concentric contractions, participants were additionally instructed to avoid any countermovement (negative/flexor torque). The real-time knee angle signal (Biodex output) was displayed on a computer monitor in front of the participants so that they could control the start of the acceleration phase.³¹

During all contractions (fixed-end and explosive), fascicle length changes were recorded (1000 Hz) by means of an ultrafast ultrasound system with a 5.5-cm linear array probe (Supersonic, Aixplorer, France). The probe was attached to the skin at approximately 50% of the femoral length, aligned with the muscle belly, and corrected with respect to the superficial and deep aponeurosis to have a clear image of the perimysial connective intramuscular tissue. Finally, VL electromyographic (EMG) activity was recorded in all contractions by means of two pairs of bipolar Ag-AgCl electrodes. The electrodes were attached over the muscle belly according to SENIAM recommendations. The raw EMG signals as well as the dynamometer torque and position signals were synchronously A/D converted at 1000 Hz using a PowerLab System (PowerLab, ADInstruments, Dunedin, New Zealand).

2.5 | Data analysis

The torque signal obtained in each contraction was low-pass-filtered at 50 Hz using a fourth-order zero-lag Butterworth filter. The total torque generated by the knee extensors was corrected for the gravitational torque effects (determined during a passive joint rotation driven by the dynamometer). After that, torque values were converted to forces using the internal moment arm as proposed by Bakenecker et al.³³ Subsequently, force onset in all contractions was defined as the point at which the first derivative of the active force–time curve crossed zero for the last time.³⁴

To obtain the knee extensor force–angle relationship, the highest value of force recorded at each knee angle was taken as the maximum force value for that angle. The optimal knee joint angle then was calculated as the angle associated with the apex of the force–angle curve as determined using a second-order polynomial relationship.

For the explosive contractions, contraction quality was monitored by an operator viewing the EMG and torque signals on LabChart software. Five maximal contractions in which the knee joint angle 75 ms after onset was closest to the target angle were selected for further analyses for each contraction condition. The knee joint angle at which peak knee extensor force was produced was reached in both contractions at 75 ms after force onset, as requested (Figure S1). Therefore, the data were analyzed up to this specific time point (0–75 ms after force onset) and were also analyzed from 75 to 150 ms after force onset to better understand the differences in fascicle dynamics imposed by both contraction conditions during more extended time phases. Therefore, all data refer to a specific phase: 0–75 and 75–150 ms after force onset.

RFD was calculated as the first derivative of the filtered force–time signal for both contractions. Mean RFD between 0–75 and 75–150 ms after force onset were calculated and used for analyses. EMG signals were filtered with a band-pass fourth-order Butterworth filter at 20–450 Hz, and onset of muscle activity was detected using visual, systematic inspection, as suggested by Tillin et al.^{35,36} During each contraction condition, the VL root mean squared EMG amplitude was measured using a symmetric, moving average time window of 10 ms from EMG onset to 150 ms. The EMG signal as determined in the explosive contractions was normalized to the maximum EMG amplitude recorded during a maximum voluntary isometric contraction. Normalized EMG was reported as the mean RMS amplitude measured from 0–75 and 75–150 ms relative to force onset.

Resting muscle architecture was determined when the subject was seated on the dynamometer (with the knee and hip angle at 90° and 80°, respectively) prior to the first contraction. This position better represented the geometrical characteristics of the muscle before contraction compared to the standard prone position.

Ultrasound videos of resting architecture and during each contraction were analyzed by means of a validated semi-automatic software (UltraTrack v.5.5).^{37,38} Muscle thickness was calculated as the perpendicular distance between the aponeuroses, while pennation angle was calculated as the mean fascicle insertion angles to the upper and lower aponeuroses. Fascicle length was calculated as muscle thickness/sine (pennation angle). The fascicle length data were then filtered with a low-pass, fourth-order Butterworth filter at 10 Hz. Based on the filtered ultrasound data, fascicle velocity (vf) was calculated as the ratio between the change in fascicle length and the changes in time ($\Delta L/\Delta t$), whereas the muscle belly velocity (vb) was calculated as the ratio between the change in belly length (obtained as fascicle length $\cos \alpha$, where α was the pennation angle) and the change in time ($\Delta L_b/\Delta t$).

Architectural gearing was calculated as the ratio between belly velocity and fascicle velocity.³⁹ Similar to RFD and EMG activity, fascicle velocity, muscle belly velocity, and architectural gear reached between 0–75 and 75–150 ms after force onset were collected for subsequent statistical analysis.

2.6 | Statistical analysis

All statistical analysis were performed in SPSS (version 25, IBM Corporation, Chicago, IL). Descriptive statistics were presented as group means with standard deviations. Paired *t*-testing was used to test for differences between the contractions in muscle geometry, fascicle dynamics, and muscle activation or kinetic outcomes. Differences between contraction conditions were assessed to aid interpretation of the differences in the relationships between muscle architecture and RFD between differing contraction modalities. Normality of the residuals was confirmed visually using histograms and Q-Q plots.

Pearson's correlation coefficients were used to analyze linear relationships between parameters (e.g., muscle architecture and RFD) within each contraction condition and were considered <0.1, trivial; 0.1–0.29, weak; 0.3–0.49, moderate; 0.5–0.69, strong; 0.7–0.89, very strong; >0.9 excellent.⁴⁰ Hotelling's test was used to test for differences in correlation coefficients (i.e., differences in relationships between muscle architecture and RFD) between dynamic and isometric contractions. A *p*-value of ≤ 0.05 was considered statistically significant (two-tailed testing).

3 | RESULTS

3.1 | Descriptives and comparison between conditions

VL muscle thickness, pennation angle, and fascicle length at rest were as follows: 2.5 ± 0.4 cm, $17.3 \pm 3.6^\circ$, and 9.8 ± 0.5 cm, respectively. VL geometry, fascicle dynamics, and EMG and kinetic outcomes are reported in Table 1. Muscle thickness increased during all contractions as compared to rest. The change in muscle thickness was not detectibly different between the 0–75 and 75–150 ms time windows in the isometric contraction while the change relative to rest decreased between these time windows in the dynamic contraction. Muscle thickness increased significantly more during the dynamic contraction from 0–75 ms but not 75–150 ms. Pennation angle also increased during all contractions. In both contractions, the change in pennation angle was larger from 75–150 ms than 0–75 ms. Pennation angle also increased significantly

TABLE 1 Vastus lateralis geometric changes, fascicle dynamics, and kinetic data during isometric and dynamic concentric ($2000^{\circ}\text{s}^{-2}$) contractions from 0–75 and 75–150 ms after torque onset. Values are mean \pm SD.

| | ISO 0–75 ms | DYN 0–75 ms | ISO 75–150 ms | DYN 75–150 ms |
|---|-------------------------|-------------------------|-------------------------|-------------------------|
| Muscle geometry | | | | |
| Δ Thickness (cm) | $0.12 \pm 0.03^*$ | $0.17 \pm 0.04^{##,*}$ | 0.12 ± 0.04 | $0.13 \pm 0.04^{\#}$ |
| Δ Pennation ($^{\circ}$) | $2.37 \pm 0.62^{##,**}$ | $5.99 \pm 1.33^{##,**}$ | $4.13 \pm 0.76^{##,**}$ | $8.63 \pm 0.90^{##,**}$ |
| Fascicle dynamics | | | | |
| Δ Fascicle length (cm) | $1.52 \pm 0.21^{##,*}$ | $1.58 \pm 0.23^{##,*}$ | $1.68 \pm 0.31^{##,*}$ | $1.76 \pm 0.34^{##,*}$ |
| v_f (cm s^{-1}) | $20.3 \pm 2.5^{##,*}$ | $21.1 \pm 2.7^{##,*}$ | $22.4 \pm 3.3^{##,*}$ | $23.4 \pm 3.6^{##,*}$ |
| v_b (cm s^{-1}) | $23.5 \pm 2.8^{##,*}$ | $25.3 \pm 3.0^{##,*}$ | $24.8 \pm 3.5^{##,*}$ | $26.9 \pm 3.8^{##,*}$ |
| Architectural gear | $1.16 \pm 0.4^{##,**}$ | $1.20 \pm 0.3^{##,**}$ | $1.11 \pm 0.3^{##,**}$ | $1.15 \pm 0.4^{##,**}$ |
| EMG and kinetics | | | | |
| EMG _{rms} (%EMG _{max}) | 99 ± 3 | 98 ± 5 | 96 ± 6 | 95 ± 7 |
| Torque (Nm) | $79 \pm 6^{###}$ | $67 \pm 9^{###}$ | $166 \pm 19^{###,*}$ | $147 \pm 14^{###,*}$ |
| RFD (Ns^{-1}) | $1086 \pm 100^{##,*}$ | $893 \pm 84^{##,*}$ | $1036 \pm 93^{##,*}$ | $850 \pm 89^{##,*}$ |

Significant difference between the two time points *within* each contraction. [#]Reflects $p < 0.05$, ^{##}reflects $p < 0.01$, ^{###}reflects $p < 0.001$.

Significant difference between contractions at the same time point. *Reflects $p < 0.05$, **reflects $p < 0.01$, ***reflects $p < 0.001$.

more during both time windows in the dynamic than the isometric contraction.

Fascicle and muscle belly velocities were significantly higher during 75–150 ms than 0–75 ms in both conditions and were also higher in the dynamic contraction at both time windows. Architectural gear was lower during 75–150 ms in both contractions than during the 0–75 ms. However, during both time windows, gear was significantly higher in the dynamic than the isometric contraction.

EMG amplitude did not differ between the time windows within each contraction and did not differ between contraction at any time window. Joint torque was higher during 75–150 ms than 0–75 ms in both contractions. As intended, joint torque did not differ between contractions from 0–75 ms while it was significantly greater in the isometric contraction from 75 to 150 ms. RFD was lower from 75–150 ms than 0–75 m for both contraction conditions and remained faster in isometric than dynamic contractions when assessed at both time windows.

3.2 | Correlations and comparison between isometric and dynamic conditions

Resting fascicle length and muscle thickness were not significantly correlated with RFD in both contraction types

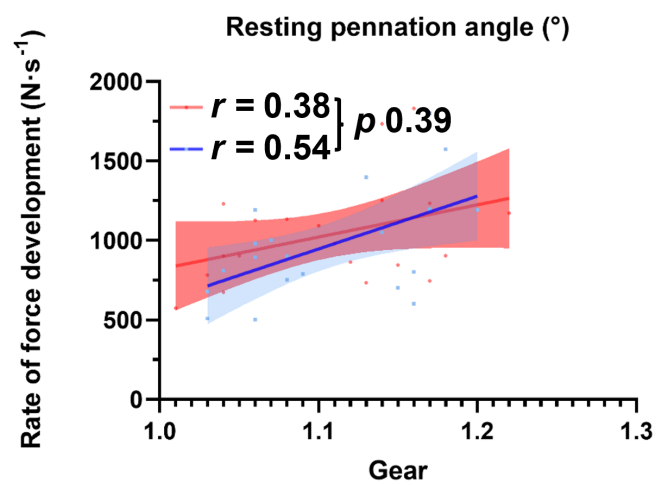
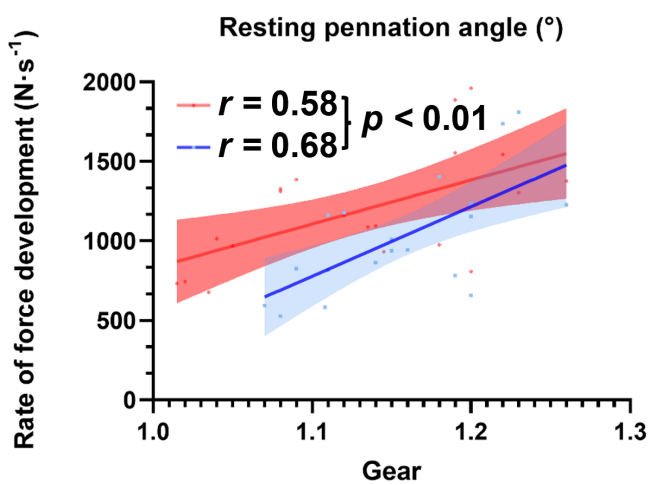
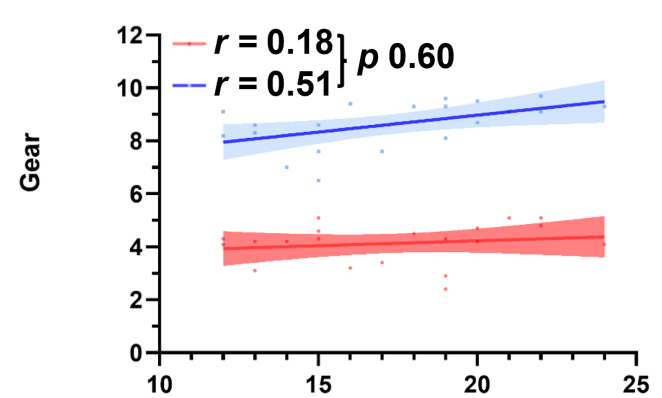
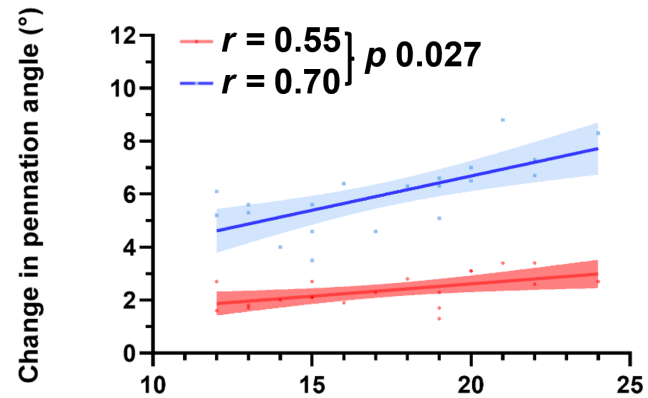
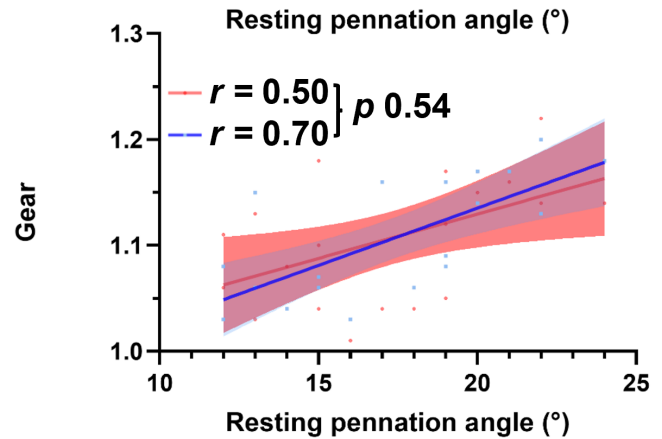
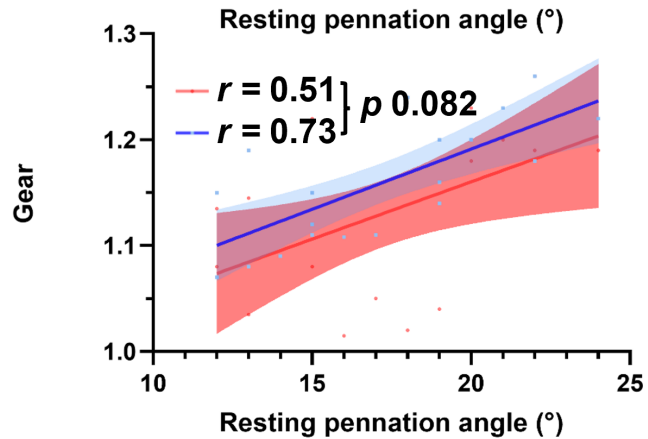
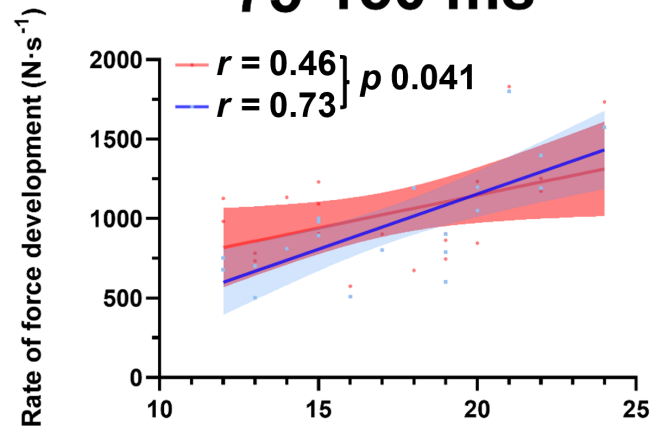
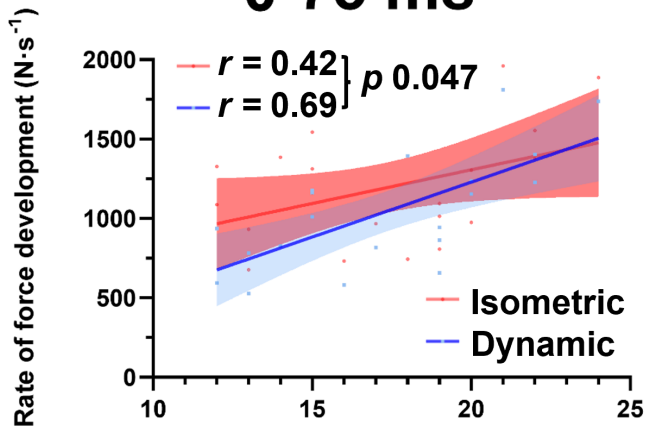
and time windows (correlation coefficients ranged from 0.25 to 0.31), see [Table S1](#) for all correlations.

Resting fascicle angle was correlated with RFD during the fixed-end ($r = 0.42$ and 0.46 at 0–75 and 75–150 ms, respectively) and dynamic contractions ($r = 0.69$ and 0.73 at 0–75 and 75–150 ms) at both time points. Resting fascicle angle was more strongly correlated with RFD during dynamic than isometric muscle actions during both time periods ($p = 0.047$ and 0.041 at 0–75 and 75–150 ms, respectively; [Figure 2](#), top row). Resting fascicle angle was correlated with architectural gear during both the fixed-end ($r = 0.51$ and 0.50 at 0–75 and 75–150 ms, respectively) and dynamic ($r = 0.73$ and 0.70 at 0–75 and 75–150 ms, respectively) contractions. These correlations did not differ significantly between contraction conditions ($p = 0.82$ and 0.54 at 0–75 and 75–150 ms, respectively; [Figure 2](#), second row). Resting fascicle angle was positively correlated with the changes in fascicle angle during the fixed-end contraction ($r = 0.55$ and 0.18 at 0–75 and 75–150 ms, respectively) while also correlated during dynamic contraction conditions ($r = 0.70$ and 0.51 at 0–75 and 75–150 ms, respectively). Resting fascicle angle was more strongly correlated with the change in fascicle angle during dynamic contraction at 0–75 ms but not at 75–150 ms ($p = 0.027$ and 0.60 at 0–75 and 75–150 ms, respectively; [Figure 2](#), third row).

FIGURE 2 Correlations between resting pennation angle and rate of force development (top), resting pennation angle and architectural gear (second row), resting pennation angle and the change in pennation angle during contraction (third row), and architectural gear and rate of force development (fourth row). Increases in resting pennation angle and gear were correlated with increases in RFD in both contractions. Stronger relationships between resting pennation angle and RFD, or gear and RFD (only during 0–75 ms) were observed for the dynamic than isometric contraction. Correlations for each contraction and the p -value of the comparison between the correlations are depicted in the figure. Each dot represents one individual during the isometric (red) or dynamic (blue) contraction.

0-75 ms

75-150 ms



Architectural gear was correlated with peak RFD during fixed-end ($r=0.58$ and 0.38 at $0-75$ and $75-150$ ms, respectively) and dynamic contractions ($r=0.68$ and 0.54 at $0-75$ and $75-150$ ms, respectively). Architectural gear was more strongly correlated with RFD during the dynamic contraction at $0-75$ ms, but not at $75-150$ ms ($p < 0.01$ and 0.39 at $0-75$ and $75-150$ ms, respectively; [Figure 2](#), bottom row).

4 | DISCUSSION

This study examined the relationship between resting skeletal muscle architecture and gearing ratio, respectively, on RFD in dynamic and isometric (fixed-end) contraction conditions. To achieve this, we first examined the relationship between fascicle angle and RFD *within* each contraction condition, finding these were moderately to very strongly correlated ([Figure 2](#)). In line with the primary study hypothesis, resting fascicle angle appeared to be more strongly correlated with RFD in the dynamic than in fixed-end, isometric test contractions during both time periods ([Figure 2](#), top row). We also hypothesized that resting fascicle angle would be more strongly correlated with RFD in the dynamic contraction due its effect on gearing. In support of this hypothesis, architectural gear ratio was higher in the dynamic vs. isometric contractions, where gear was moderately to strongly positively associated with RFD in the former condition ([Figure 2](#), bottom row). Moreover, resting fascicle angle was strongly and positively correlated with gear in both contraction conditions. Overall, these data demonstrate that larger (i.e., steeper) resting pennation angles are associated with a faster RFD compared to less pennate resting angles, which at least in part is due to enlarged architectural gear ratios.

4.1 | Differences between contraction types

Our experimental design successfully ensured comparable knee extensor torque production during both contractions at the first time point, 75 ms after contraction onset ([Table 1](#)). This constancy in torque production was accompanied by greater increases in muscle thickness and pennation angle during dynamic than fixed-end contractions. The greater increases in muscle thickness and pennation angle in the dynamic contraction may in turn be a consequence of the larger change in muscle-tendon unit length due to knee joint extension as opposed to the smaller muscle-tendon unit length change in the isometric condition as a consequence of the fixed

knee joint angle. The larger muscle-tendon unit shortening also facilitated a greater fascicle shortening velocity, which was higher by 0.8 cm s^{-1} in the dynamic contraction. However, the larger change in pennation angle in the same time frame resulted in an even greater difference in muscle belly shortening velocity (by 1.8 cm s^{-1}), revealing a higher architectural gear ratio during dynamic contractions ([Table 1](#)). Despite this higher gearing, RFD was slower in the dynamic contraction, likely as a consequence of the faster fascicle shortening velocity, which resulted in reduced force production in accordance with the hyperbolic force-velocity relationship.⁴ Nevertheless, these findings suggest that gearing can more readily offset the reduction in force that occurs with greater muscle shortening velocities in dynamic contractions as opposed to isometric contractions.

From 75 to 150 ms, both torque production and RFD were higher in the fixed-end contraction condition ([Table 1](#)). Although the observed changes in pennation angle, fascicle velocity, muscle belly velocity, and gear ratio were still greater in the dynamic contraction conditions, the change in muscle thickness did not differ between contraction types. The absence of differences in muscle thickness during this time phase could reflect an increased transverse force production (from the whole-muscle perspective) exerted by the fascicles. This force would pull the aponeuroses together, thereby limiting spatial changes in whole-muscle thickness (during fixed-end contractions), or even reducing muscle thickness (during dynamic contractions relative to the earlier time point; [Table 1](#)). Despite the similar between-condition increases in muscle thickness during $75-150$ ms relative to rest, the increase in pennation angle was still greater in the dynamic contraction, probably as a result of the greater longitudinal muscle shortening (and shortening velocity) allowed by the knee extension.

Previous studies examining isotonic fixed-end contractions have observed decreased gear ratios with increasing muscle force.^{20,23,41} In line with these observations, we also found decreased gear ratios in both contraction conditions at the later $75-150$ ms time window, when force production was higher and RFD lower than at $0-75$ ms ([Table 1](#)). These observations lend further support to the notion that architectural gearing is inversely modulated by the level of active force generation.^{20,26}

4.2 | Correlation analysis

We hypothesized that differences in both muscle geometry and fascicle dynamics between the contractions could impact the relationship between resting muscle architecture and RFD. We found that fascicle angle and RFD were

moderately to very strongly correlated in both conditions (Figure 2). However, in line with our hypothesis, resting fascicle angle was more strongly correlated with RFD in the dynamic than in the fixed-end contraction during both time windows (Figure 2, top row). The stronger correlation between resting fascicle angle and RFD in the dynamic contraction may primarily reflect the smaller restrictions on muscle shape change in the dynamic contraction than the isometric contraction. Specifically, the greater longitudinal shortening in the dynamic contraction may have allowed for larger changes in pennation, thus increasing the correlation between resting fascicle angle and RFD. Indeed, while differences in fascicle/fiber force can also impact gearing,^{20,26} force production was identical between isometric and dynamic contraction conditions during this particular time window. This suggests that the level of force exertion did not contribute to the differences in the observed correlations. Similarly, while RFD was higher during both time windows in the isometric contraction than the dynamic contraction (Table 1), the magnitude of this difference would be too small to substantially influence the stiffness of elastic tissues via viscous effects,^{42,43} thus making it unlikely that this impacted the observed correlations.

We hypothesized that a larger resting fascicle angle would correlate with greater RFD via higher architectural gearing. In support of this hypothesis, architectural gear was moderately to strongly positively correlated with RFD (Figure 2, bottom row) while resting fascicle angle was strongly correlated with gear in both contraction conditions (Figure 2, second row). Mechanistically, the

higher gear allows the fascicle to operate at higher force-velocity potential, without compromising the overall origin-insertion muscle shortening velocity. The positive correlation between resting fascicle angle and architectural gear (and RFD) observed in the present study in turn indicates that a given change in fascicle angle results in a larger change in belly/muscle length (or velocity) with higher resting fascicle angles, as shown in Figure 3. In other words, higher resting fascicle angles allow the muscle to operate at a higher gear, which in turn allows the fascicles to operate at a higher force-velocity potential. Importantly, the combination of higher fascicle force-velocity potential and a higher overall muscle contraction velocity increases the mechanical power produced by the muscle-tendon unit at a given shortening velocity.

4.3 | Study limitations

A number of limitations should be considered when interpreting the present findings. First, muscle geometry and fascicle dynamics were assessed only in the VL. Although the VL is considered a primary knee extensor due to its large cross-sectional area,⁴⁴ other quadriceps compartments also contribute to the knee extensor moment. Secondly, the use of 2D ultrasonography represents a simplified approach compared to the complex 3D architecture of the vastus lateralis,⁴⁵ and the general 3D behavior of muscles during contraction.³⁷ For example, gearing can occur in both the sagittal and coronal plane,⁴⁶ whereas only sagittal-plane

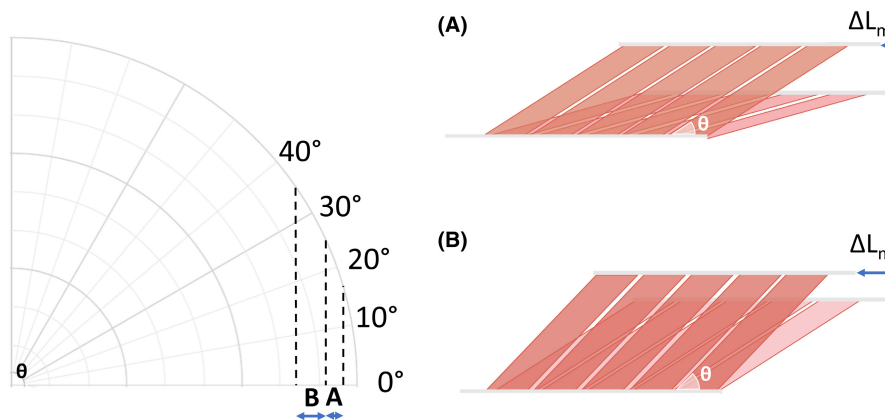


FIGURE 3 Schematic illustration of the effect of resting pennation angle on architectural gear using a simplistic 2D muscle model. Muscles A and B differ in resting pennation angles: 15° for muscle A and 25° for muscle B (in line with the resting angles in our sample²⁵). Upon contraction, both muscles increase their pennation angle by 10° due to transverse fascicle expansion (notice the shortening and thickening of the schematic fascicles). The muscle with higher resting pennation angle will shorten further (change in muscle length, L_m) since the pennation change will more effectively contribute to the change in muscle length (enlarged projection). This is also illustrated in the polar plot on the left, with muscle A exhibiting a rather small decrease in muscle length when pennation increases from 15° to 25°, while muscle B shows a larger decrease in muscle length when pennation angle increases by the same absolute amount, from 25° to 35°. Greater resting pennation angles should therefore benefit overall muscle shortening velocity due to the higher resulting architectural gear adopted during dynamic contraction.

gearing was examined in the present study. Related to this, we determined gearing by calculating belly velocity using trigonometric equations based on one fascicle. However, belly segment and whole belly gearing may differ.²² Although this may affect the absolute gear magnitude, it is unlikely to influence our comparison between conditions because the same approach was used for both contractions. Future studies may explore whether the observed differences are also found when using whole belly gearing. Thirdly, the present experimental set-up allowed the knee extensors and thereby VL to operate at the same torque-angle potential and reach the same torque values at 75 ms after force onset in both contractions. However, minor changes in starting position could have influenced the stiffness of elastic structures in the first milliseconds of contraction, which in turn could have affected RFD by altering fascicle contraction velocity. Nevertheless, these differences are expected to be negligible because knee angle (75° vs. 76°), and VL pennation angle (17.9° vs. 18.4°) differences at torque onset were minimal for the isometric and dynamic contractions, respectively. Moreover,

the impact of such differences is further reduced when examining relatively longer time windows (from 0 to 75 ms and from 75 to 150 ms), as in the present study. Finally, we tested the differences between fixed-end and dynamic contractions using a single, fixed rate of joint angular acceleration. We selected $2000^{\circ}\text{s}^{-2}$ to match the torque level at 75 ms to that observed during the fixed-end contractions. Future studies should investigate the generalizability of the present findings to other accelerations.

4.4 | Perspectives and implications

There are several potential implications of the present observations. Firstly, our findings suggest that muscle length change restrictions during fixed-end contractions, as commonly examined in previous studies, may affect the relationship between muscle architecture and RFD. This might at least in part explain the previous conflicting presence or lack of relationships between measures of muscle architecture and RFD.⁴⁻⁸ Studies

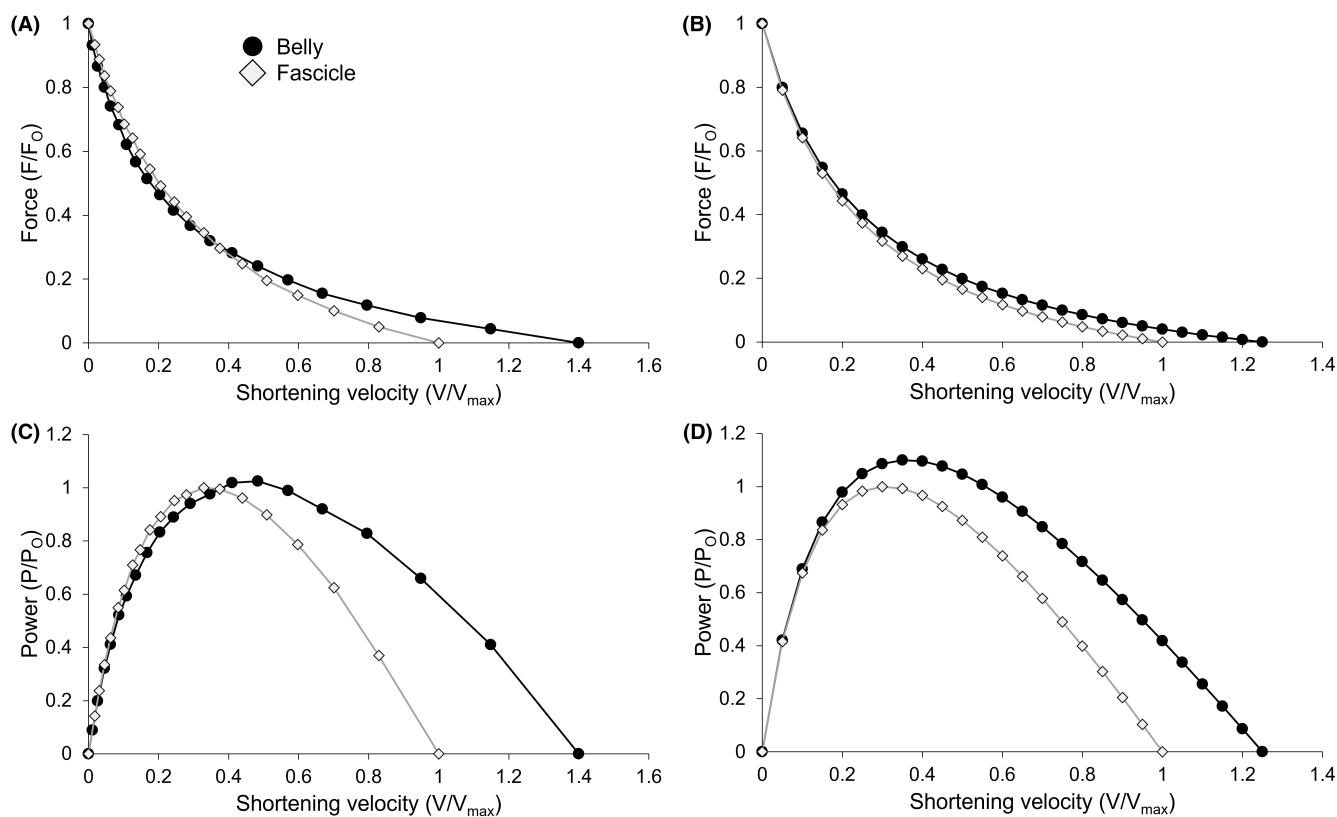


FIGURE 4 VL belly (closed symbols) and fascicle (open symbols) force–velocity relations (upper panels) and power–velocity relations (lower panels) from Azizi, Brainerd, and Roberts²⁰ (Panels A and C) and the present study (original data from Monte, Bertucco, Magris, and Zamparo²⁵; Panels B and D). All axis variables are scaled relative to the fascicle maximum. Note that for a given muscle force, the belly can contract at a faster shortening velocity than the fascicle in both datasets (upper panels). This translates into a rightward shift and broadening of the power–velocity relation, where peak power is attained at a higher velocity and more power can be produced at incrementally faster velocities (lower panels).

investigating the morphologic and neural contributions to RFD should therefore strongly consider the use of dynamic explosive-type test settings to allow for the muscle shape changes that are expected in some activities of daily living and sporting tasks. Within this context, it is, however, important to consider that movements in daily living or sports are rarely initiated from complete rest and may not always involve a large range of muscle shortening, even in dynamic movements such as running (e.g., ref. [47]). Nevertheless, the use of dynamic explosive-type test may further improve our understanding of the contribution of muscle fiber/fascicle behavior to force production, and provide a deeper understanding of its influence on architectural gearing and mechanical muscle function during dynamic activities involving substantial muscle shortening (e.g., sprint start and vertical jump). Such experimental approaches may also provide important insights into the relative importance of neural, morphological, and architectural variables to RFD in such activities.

Second, trivial-to-weak correlations between isometric and dynamic measures of RFD (during for example vertical jumping) typically have been attributed to differences in coordination or the adopted joint angles (e.g., ref. [48]). However, the present findings suggest that contraction-specific differences in muscle shape changes and thus architectural gearing between dynamic and isometric contractions may also, at least partly, underpin these differences.

Thirdly, the passive stiffness of intra- and extra-muscular connective tissues as well as epimuscular connective tissues (e.g., aponeurosis and muscle fascia) are likely to influence the gear magnitude and thus affect RFD as well as force- and velocity-specific muscle power outputs. Tissue stiffness may change with training, aging, disuse, or injury, and could therefore influence contractile performance by altering the magnitude of architectural gearing, with this effect possibly varying between isometric and dynamic contraction conditions. Along this line of reasoning, the specific experimental set-up could represent a possible confounding factor for data interpretation. For example, straps used for limb stabilization during dynamometry assessment and for fixing ultrasound probes for muscle imaging may result in external compression^{21,49,50} and thereby restrict the magnitude of muscle shape change and thereby limit RFD. Indeed, *in vivo* and *in situ* studies have shown that muscle compression can influence RFD.^{49,51} Straps should therefore be placed such that they allow the muscle to freely change shape.

Fourthly, the present data may also be important for the development and validation of muscle models that

predict 3D muscle deformation and related changes in muscle architecture during actual movement.^{52,53}

Finally, numerous studies have reported changes (increases) in muscle fascicle pennation following resistance exercise training interventions (e.g., refs [54–56]). While the practical outcomes of such adaptations have traditionally been considered from the perspective of increased maximal muscle force potential, our findings suggest this adaptation may also enhance the rate at which force can be developed (RFD) through its effect on increasing gearing, which may be more readily reflected in dynamic as opposed to isometric test conditions. For example, according to our data (Figure 2), a 10% increase in resting fascicle angle may be associated with a 1.69% increase in gear ratio and a 11.5% to 12.5% increase in RFD in dynamic contractions, with less effect (1.30% to 1.65% and 6.16% to 6.90%, respectively) in isometric contractions (note that the exact effect will likely differ for other muscles and under different contractile conditions). To further illustrate the beneficial effects of optimized gearing, Figure 4 depicts the relationship between muscle (belly) and fascicle force and origin-insertion velocity, and the corresponding power output. From this figure, it can be seen that the muscle as a whole can produce a higher force, in particular at higher origin-insertion shortening velocities, than it otherwise would, as a result of architectural gearing. Consequently, average whole-muscle power output is higher at faster shortening velocities compared to fascicle power output. Dynamic changes in architecture during contraction can therefore allow muscles to partially circumvent the limitations imposed by the force–velocity relation of the fibers,²⁰ and this can result in higher levels of force and power production at a given origin-insertion muscle shortening speed.

5 | CONCLUSION

Greater (steeper) resting VL fascicle angles were positively correlated with peak rate of torque development during both isometric and dynamic concentric knee extensor contractions. These correlations were, however, stronger during the dynamic contractions during both investigated time windows. Greater resting VL fascicle angles also correlated with increased architectural gearing ratios during both contractions, with this correlation again being stronger in the dynamic condition, at least during the first 75 ms of contractions (i.e., in the early phase of muscle shortening for dynamic contractions). As a result, architectural gearing also showed a stronger relationship with rate of force development during the dynamic contraction. Our findings suggest that differences in the contribution of resting muscle architecture

and architectural gearing between isometric and dynamic muscle contractions may stem from geometric restrictions imposed on muscle shape changes during isometric contractions.

FUNDING INFORMATION

None.

CONFLICT OF INTEREST STATEMENT

The authors declare no conflicts of interest.

DATA AVAILABILITY STATEMENT

The data that support the findings of this study are available from the corresponding author upon reasonable request.

ORCID

Bas Van Hooren  <https://orcid.org/0000-0001-8163-693X>

Per Aagaard  <https://orcid.org/0000-0002-9773-7361>

Andrea Monte  <https://orcid.org/0000-0001-6604-2658>

Anthony J. Blazevich  <https://orcid.org/0000-0003-1664-1614>

REFERENCES

1. Van Hooren B, Bosch F, Meijer K. Can resistance training enhance the rapid force development in unloaded dynamic isoinertial multi-joint movements? A systematic review. *J Strength Cond Res*. 2017;31(8):2324-2337. doi:10.1519/JSC.0000000000001916
2. Maffiuletti NA, Aagaard P, Blazevich AJ, Folland J, Tillin N, Duchateau J. Rate of force development: physiological and methodological considerations. *Eur J Appl Physiol*. 2016;116(6):1091-1116. doi:10.1007/s00421-016-3346-6
3. Rodriguez-Rosell D, Pareja-Blanco F, Aagaard P, Gonzalez-Badillo JJ. Physiological and methodological aspects of rate of force development assessment in human skeletal muscle. *Clin Physiol Funct Imaging*. 2018;38(5):743-762. doi:10.1111/cpf.12495
4. Raiteri BJ, Hahn D. A reduction in compliance or activation level reduces residual force depression in human tibialis anterior. *Acta Physiol (Oxf)*. 2019;225(3):e13198. doi:10.1111/apha.13198
5. Morl F, Siebert T, Haufle D. Contraction dynamics and function of the muscle-tendon complex depend on the muscle fibre-tendon length ratio: a simulation study. *Biomech Model Mechanobiol*. 2016;15(1):245-258. doi:10.1007/s10237-015-0688-7
6. Zaras ND, Stasinaki AN, Methenitis SK, et al. Rate of force development, muscle architecture, and performance in young competitive track and field throwers. *J Strength Cond Res*. 2016;30(1):81-92. doi:10.1519/JSC.0000000000001048
7. Coratella G, Longo S, Borrelli M, Doria C, Ce E, Esposito F. Vastus intermedius muscle architecture predicts the late phase of the knee extension rate of force development in recreationally resistance-trained men. *J Sci Med Sport*. 2020;23(11):1100-1104. doi:10.1016/j.jsams.2020.04.006
8. Maden-Wilkinson TM, Balshaw TG, Massey GJ, Folland JP. Muscle architecture and morphology as determinants of explosive strength. *Eur J Appl Physiol*. 2021;121(4):1099-1110.
9. Wagle JP, Carroll KM, Cunanan AJ, et al. Comparison of the relationship between lying and standing ultrasonography measures of muscle morphology with isometric and dynamic force production capabilities. *Sports*. 2017;5(4):88. doi:10.3390/sports5040088
10. Randhawa A, Jackman ME, Wakeling JM. Muscle gearing during isotonic and isokinetic movements in the ankle plantarflexors. *Eur J Appl Physiol*. 2013;113(2):437-447. doi:10.1007/s00421-012-2448-z
11. Werkhausen A, Gloersen O, Nordez A, Paulsen G, Bojsen-Moller J, Seynnes OR. Rate of force development relationships to muscle architecture and contractile behavior in the human vastus lateralis. *Sci Rep*. 2022;12(1):21816. doi:10.1038/s41598-022-26379-5
12. Reinhardt L, Siebert T, Leichsenring K, Blickhan R, Bül M. Intermuscular pressure between synergistic muscles correlates with muscle force. *J Exp Biol*. 2016;219(15):2311-2319.
13. Brainerd EL, Azizi E. Muscle fiber angle, segment bulging and architectural gear ratio in segmented musculature. *J Exp Biol*. 2005;208(Pt 17):3249-3261. doi:10.1242/jeb.01770
14. Hauraix H, Nordez A, Guilhem G, Rabita G, Dorel S. In vivo maximal fascicle-shortening velocity during plantar flexion in humans. *J Appl Physiol (1985)*. 2015;119(11):1262-1271. doi:10.1152/jappphysiol.00542.2015
15. Hauraix H, Dorel S, Rabita G, Guilhem G, Nordez A. Muscle fascicle shortening behaviour of vastus lateralis during a maximal force-velocity test. *Eur J Appl Physiol*. 2017;117(2):289-299. doi:10.1007/s00421-016-3518-4
16. Kubo K. Maximal fascicle shortening velocity measurements in human medial gastrocnemius muscle in vivo. *Physiol Rep*. 2023;11(1):e15541. doi:10.14814/phy2.15541
17. Herbert RD, Bolsterlee B, Gandevia SC. Passive changes in muscle length. *J Appl Physiol (1985)*. 2019;126(5):1445-1453. doi:10.1152/jappphysiol.00673.2018
18. Gans C. Fiber architecture and muscle function. *Exerc Sport Sci Rev*. 1982;10(1):160-207.
19. Gans C, de Vree F. Functional bases of fiber length and angulation in muscle. *J Morphol*. 1987;192(1):63-85. doi:10.1002/jmor.1051920106
20. Azizi E, Brainerd EL, Roberts TJ. Variable gearing in pennate muscles. *Proc Natl Acad Sci USA*. 2008;105(5):1745-1750. doi:10.1073/pnas.0709212105
21. Monte A. In vivo manipulation of muscle shape and tendinous stiffness affects the human ability to generate torque rapidly. *Exp Physiol*. 2021;106(2):486-495. doi:10.1113/EP089012
22. Pinto MD, Nosaka K, Wakeling JM, Blazevich AJ. Human in vivo medial gastrocnemius gear during active and passive muscle lengthening: effect of inconsistent methods and nomenclature on data interpretation. *Biol Open*. 2023;12(9):bio060023. doi:10.1242/bio.060023
23. Holt NC, Danos N, Roberts TJ, Azizi E. Stuck in gear: age-related loss of variable gearing in skeletal muscle. *J Exp Biol*. 2016;219(Pt 7):998-1003. doi:10.1242/jeb.133009
24. Eng CM, Azizi E, Roberts TJ. Structural determinants of muscle gearing during dynamic contractions. *Integr Comp Biol*. 2018;58(2):207-218. doi:10.1093/icb/icy054

25. Monte A, Bertuccio M, Magris R, Zamparo P. Muscle belly gearing positively affects the force-velocity and power-velocity relationships during explosive dynamic contractions. *Front Physiol.* 2021;12:683931. doi:10.3389/fphys.2021.683931
26. Dick TJM, Wakeling JM. Shifting gears: dynamic muscle shape changes and force-velocity behavior in the medial gastrocnemius. *J Appl Physiol (1985).* 2017;123(6):1433-1442. doi:10.1152/japplphysiol.01050.2016
27. Sleboda DA, Roberts TJ, Azizi E. Architectural gear ratio depends on actuator spacing in a physical model of pennate muscle. *Bioinspir Biomim.* 2024;19(2):026007.
28. Kelp NY, Clemente CJ, Tucker K, Hug F, Pinel S, Dick TJM. Influence of internal muscle properties on muscle shape change and gearing in the human gastrocnemii. *J Appl Physiol (1985).* 2023;134(6):1520-1529. doi:10.1152/japplphysiol.00080.2023
29. Monte A, Magris R, Nardello F, Bombieri F, Zamparo P. Muscle shape changes in Parkinson's disease impair function during rapid contractions. *Acta Physiol (Oxf).* 2023;238(1):e13957. doi:10.1111/apha.13957
30. Roberts TJ, Eng CM, Sleboda DA, et al. The multi-scale, three-dimensional nature of skeletal muscle contraction. *Physiology (Bethesda).* 2019;34(6):402-408. doi:10.1152/physiol.00023.2019
31. Tillin NA, Pain MTG, Folland JP. Contraction speed and type influences rapid utilisation of available muscle force: neural and contractile mechanisms. *J Exp Biol.* 2018;221(Pt 24):jeb193367. doi:10.1242/jeb.193367
32. Sahaly R, Vandewalle H, Driss T, Monod H. Maximal voluntary force and rate of force development in humans—importance of instruction. *Eur J Appl Physiol.* 2001;85(3–4):345-350. doi:10.1007/s004210100451
33. Bakenecker P, Raiteri B, Hahn D. Patella tendon moment arm function considerations for human vastus lateralis force estimates. *J Biomech.* 2019;86:225-231.
34. Tillin NA, Pain MT, Folland JP. Contraction type influences the human ability to use the available torque capacity of skeletal muscle during explosive efforts. *Proc Biol Sci.* 2012;279(1736):2106-2115. doi:10.1098/rspb.2011.2109
35. Tillin NA, Pain MTG, Folland JP. Short-term training for explosive strength causes neural and mechanical adaptations. *Exp Physiol.* 2012;97(5):630-641. doi:10.1113/expphysiol.2011.063040
36. Tillin NA, Jimenez-Reyes P, Pain MTG, Folland JP. Neuromuscular performance of explosive power athletes versus untrained individuals. *Med Sci Sports Exerc.* 2010;42(4):781-790. doi:10.1249/MSS.0b013e3181be9c7e
37. Van Hooren B, Teratsias P, Hodson-Tole EF. Ultrasound imaging to assess skeletal muscle architecture during movements: a systematic review of methods, reliability, and challenges. *J Appl Physiol (1985).* 2020;128(4):978-999. doi:10.1152/japplphysiol.00835.2019
38. Farris DJ, Lichtwark GA. UltraTrack: software for semi-automated tracking of muscle fascicles in sequences of B-mode ultrasound images. *Comput Methods Programs Biomed.* 2016;128:111-118. doi:10.1016/j.cmpb.2016.02.016
39. Wakeling JM, Blake OM, Wong I, Rana M, Lee SSM. Movement mechanics as a determinate of muscle structure, recruitment and coordination. *Philos T R Soc B.* 2011;366(1570):1554-1564. doi:10.1098/rstb.2010.0294
40. Hopkins WG. A scale of magnitudes for effect statistics. *NewStats.* Accessed 1–3, 15. newstats.org/effectmag.html
41. Azizi E, Roberts TJ. Geared up to stretch: pennate muscle behavior during active lengthening. *J Exp Biol.* 2014;217(Pt 3):376-381. doi:10.1242/jeb.094383
42. Ker RF. Dynamic tensile properties of the plantaris tendon of sheep (*Ovis aries*). *J Exp Biol.* 1981;93(1):283-302. doi:10.1242/jeb.93.1.283
43. Rosario MV, Roberts TJ. Loading rate has little influence on tendon fascicle mechanics. *Front Physiol.* 2020;11:255. doi:10.3389/fphys.2020.00255
44. Narici MV, Roi GS, Landoni L, Minetti AE, Cerretelli P. Changes in force, cross-sectional area and neural activation during strength training and detraining of the human quadriceps. *Eur J Appl Physiol Occup Physiol.* 1989;59(4):310-319. doi:10.1007/BF02388334
45. Forsting J, Rehm R, Froeling M, Vorgerd M, Tegenthoff M, Schaffke L. Diffusion tensor imaging of the human thigh: consideration of DTI-based fiber tracking stop criteria. *MAGMA.* 2020;33:343-355.
46. Takahashi K, Shiotani H, Evangelidis PE, Sado N, Kawakami Y. Coronal as well as sagittal fascicle dynamics can bring about a gearing effect in muscle elongation by passive lengthening. *Med Sci Sports Exerc.* 2023;55(11):2035-2044. doi:10.1249/MSS.0000000000003229
47. Bohm S, Marzilger R, Mersmann F, Santuz A, Arampatzis A. Operating length and velocity of human vastus lateralis muscle during walking and running. *Sci Rep.* 2018;8(1):5066. doi:10.1038/s41598-018-23376-5
48. Van Hooren B, Kozinc Ž, Smajla D, Sarabon N. Isometric single-joint rate of force development shows trivial to small associations with jumping rate of force development, jump height, and propulsive duration in a large sample of heterogeneous individuals. *JSASM Plus.* 2023;1:1-8.
49. Wakeling JM, Jackman M, Namburete AI. The effect of external compression on the mechanics of muscle contraction. *J Appl Biomech.* 2013;29(3):360-364.
50. Randhawa A, Wakeling JM. Transverse anisotropy in the deformation of the muscle during dynamic contractions. *J Exp Biol.* 2018;221(Pt 15):jeb175794. doi:10.1242/jeb.175794
51. Stutzig N, Ryan D, Wakeling JM, Siebert T. Impact of transversal calf muscle loading on plantarflexion. *J Biomech.* 2019;85(6):37-42. doi:10.1016/j.jbiomech.2019.01.011
52. Seydewitz R, Siebert T, Bol M. On a three-dimensional constitutive model for history effects in skeletal muscles. *Biomech Model Mechanobiol.* 2019;18(6):1665-1681. doi:10.1007/s10237-019-01167-9
53. Rohrl O, Sprenger M, Schmitt S. A two-muscle, continuum-mechanical forward simulation of the upper limb. *Biomech Model Mechanobiol.* 2017;16(3):743-762. doi:10.1007/s10237-016-0850-x
54. Aagaard P, Andersen JL, Dyhre-Poulsen P, et al. A mechanism for increased contractile strength of human pennate muscle in response to strength training: changes in muscle architecture. *J Physiol.* 2001;534(2):613-623.
55. Timmins RG, Ruddy JD, Presland J, et al. Architectural changes of the biceps femoris after concentric or eccentric training. *Med Sci Sports Exerc.* 2016;48(3):499-508. doi:10.1249/MSS.0000000000000795

56. Blazevich AJ, Cannavan D, Coleman DR, Horne S. Influence of concentric and eccentric resistance training on architectural adaptation in human quadriceps muscles. *J Appl Physiol* (1985). 2007;103(5):1565-1575. doi:[10.1152/jappphysiol.00578.2007](https://doi.org/10.1152/jappphysiol.00578.2007)

SUPPORTING INFORMATION

Additional supporting information can be found online in the Supporting Information section at the end of this article.

How to cite this article: Van Hooren B, Aagaard P, Monte A, Blazevich AJ. The role of pennation angle and architectural gearing to rate of force development in dynamic and isometric muscle contractions. *Scand J Med Sci Sports*. 2024;34:e14639. doi:[10.1111/sms.14639](https://doi.org/10.1111/sms.14639)